

PAPER • OPEN ACCESS

## Analysis of fuselage skin reinforcements with beam element models in flexible aircraft panels for ditching simulations

To cite this article: C Leon Muñoz *et al* 2021 *IOP Conf. Ser.: Mater. Sci. Eng.* **1024** 012054

View the [article online](#) for updates and enhancements.

# Analysis of fuselage skin reinforcements with beam element models in flexible aircraft panels for ditching simulations

C Leon Muñoz<sup>1,\*</sup>, D Kohlgrüber<sup>1</sup> and B Langrand<sup>2</sup>

<sup>1</sup> German Aerospace Center (DLR), Institute of Structures and Design (BT), Pfaffenwaldring 38-40, D-70569 Stuttgart, Germany

<sup>2</sup> ONERA – The French Aerospace Lab, Materials and Structures Department (DMAS), 5, rue des Fortifications, CS 90013, F-59014 Lille Cedex, France

\*E-mail address: christian.leonmunoz@dlr.de

**Abstract.** This paper is dedicated to the use of beam element models for skin structural reinforcements in guided ditching simulations with a flexible aircraft panel. This approach was analysed by means of finite element simulations of the structure subjected to a constant pressure load and guided ditching loading conditions. To verify this approach, finite element models of different discretization types and different mesh sizes were considered in the computations. Moreover, guided ditching simulations were enhanced by comparisons with the coupled Finite Element-Smoothed Particle Hydrodynamics and the Arbitrary Lagrangian Eulerian methods.

## 1. Introduction

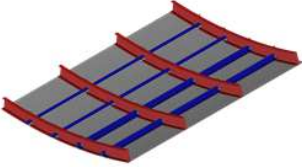
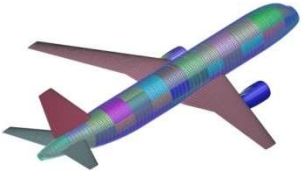
In the scope of the certification process of novel fixed-wing aircraft models aircraft manufacturers must demonstrate compliance with respect to ditching requirements for overwater operations. Ditching is a planned emergency landing on water characterized by the pre-event preparation as well as low impact velocities and a nose-up position in order to increase the survivability of the occupants [1]. One of the requirements is to demonstrate airframe structural integrity towards high hydrodynamic loads expected during impact and the subsequent landing phase. Among diverse methods used to investigate it numerical computations based on the finite element approach overhang in the possibility to provide both the global behavior of the aircraft kinematics and the local structural deformation. By using a multidisciplinary pre-design process chain for the generation of aircraft models combined with the development of appropriate analysis methods for detailed flexible structures, complex models can be integrated in ditching simulations. However, the application to full aircraft computations is challenging since very detailed discretization models are not feasible in terms of computational effort and numerical stability. Differences on selected characteristics between both approaches are presented in table 1.

To close the gap between detailed local analysis and the full aircraft application a representative flexible aircraft fuselage panel was used. In the past simple flexible generic panels were used in a guided ditching experimental test campaign to validate the numerical method for ditching simulations [2]. To extend the ditching analysis to representative aircraft structures, a reinforced panel with stringers and frames was modeled. Findings showed an increased hydrodynamic loading due to structural deformation [3-4], being consistent with the results of the generic panels. A further development of the flexible panel for the representation of reinforcement structures with beam elements is major part of this investigation.



The first part of the paper is dedicated to the description of the numerical approaches and the different discretization types and mesh sizes considered to represent the flexible aircraft panel, followed by the verification of the structural model using a constant pressure loading condition. In the next part the application of the flexible panel in guided ditching simulations is presented. Finally, conclusions of this investigation are given in the last section.

**Table 1.** Characteristics of different modelling approaches for ditching analysis.

	Detailed local analysis [3-4]	Full aircraft application [5]
		
Standard skin mesh size	10 mm	150 mm
Modelling method for skin reinforcements	Cross-section extruded (shell elements)	Representation with engineering constants (beam elements)
Number of elements	15320	50981
Fluid particle size	10 mm	200 mm
Physical time	~ 9 h for 85 ms with 32 CPUs	~12 h for 1000 ms with 32 CPUs

## 2. Numerical approaches

The transient interaction of fluid and structure is computed in a coupled manner by using an explicit time integration scheme. In this work the structure is modeled using the Finite Element (FE) method and a lagrangian formulation for the mesh and material deformation. This is conventional practice for structural representations in crashworthiness applications.

Since ‘large’ deformations are expected in the fluid due to the high hydrodynamic loads the mesh-free lagrangian method so-called Smoothed Particle Hydrodynamics (SPH) is used. The fluid domain is discretized by a series of particles. This method is commonly used in this type of application [6]. To reduce computational effort and numerical instabilities the volume surrounding the SPH domain was discretized with FE, giving the fluid model a hybrid definition. To couple SPH and FE a node-to-surface penalty contact formulation is used [7].

Further, the eulerian formulation is commonly used for computations in fluid dynamics simulations. The material is moving independently in the fixed mesh. In combination with the lagrangian formulation (as for the structure), the Arbitrary Lagrangian-Eulerian (ALE) method allows for the arbitrary motion of the mesh points with respect to a fixed frame, thus combining the advantages of both methods [8]. To enhance the comparability of methods in this investigation, the ALE formulation will be included in the analysis. The coupling of fluid and structure relies on the use of an embedded interface. Due to the fact that the lagrangian structure is immersed in the eulerian fluid domain, this type of fluid-structure interaction approach is called Coupled Euler-Lagrange (CEL) method.

## 3. Modelling technics of the structural model

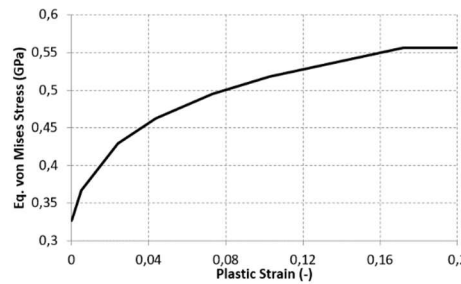
A generic flexible reinforced lower aircraft panel, similar to a panel of the rear bottom fuselage section, was developed [3]. The panel consists of a thin skin surface reinforced with extruded stringers and frames, which are connected with clips using tied interfaces and are riveted to the skin (figure 1). Stringers and frames are modelled with shell FE to represent a Z-profile and a C-profile respectively. Moreover, outer frames are supposed quasi-rigid structural parts. This is done by increasing the FE thickness. This model is taken as reference for the comparisons with the results obtained with the simplified models.

### 3.1. Material model

The mechanical behavior of the material is isotropic elastic-plastic. The properties correspond to an aluminum alloy AL2024, which is widely used in fuselage structures. The tabulated curve in table 2 is used for the isotropic hardening. Material inputs are density  $2.8 \times 10^{-6} \text{ kgmm}^{-3}$ , Young modulus 72.14 GPa, Poisson ratio 0.33, and initial yield stress 0.3268 GPa.

**Table 2.** Values of the isotropic hardening model and stress-plastic strain curve.

Plastic Strain (-)	Stress (GPa) Tabulated Curve
0	0.3268
0.004928	0.3665
0.024595	0.4296
0.043591	0.4625
0.073122	0.4950
0.102763	0.5183
0.172315	0.5566



### 3.2. Model discretization

The reference model uses a mesh that has non-conformal interfaces. As a first step, a simplified shell-stiffened flexible panel made of skin and reinforcements that have a conformal mesh (common nodes) is obtained to reduce the complexity of the mesh generation. In this simplified model, connections, most of the contact interfaces and mouseholes are excluded. To consider stringer and frame flanges the skin thickness was updated in the related areas.

In a next step, stringers and inner frames are replaced by beam finite elements. Mechanical properties including moments of inertia, torsion and warping constant as well as the center of gravity position are calculated with a proprietary FEM code using the cross-section geometry of the profiles. Figure 1 depicts the flexible reinforced aircraft panel for the different simplification steps.

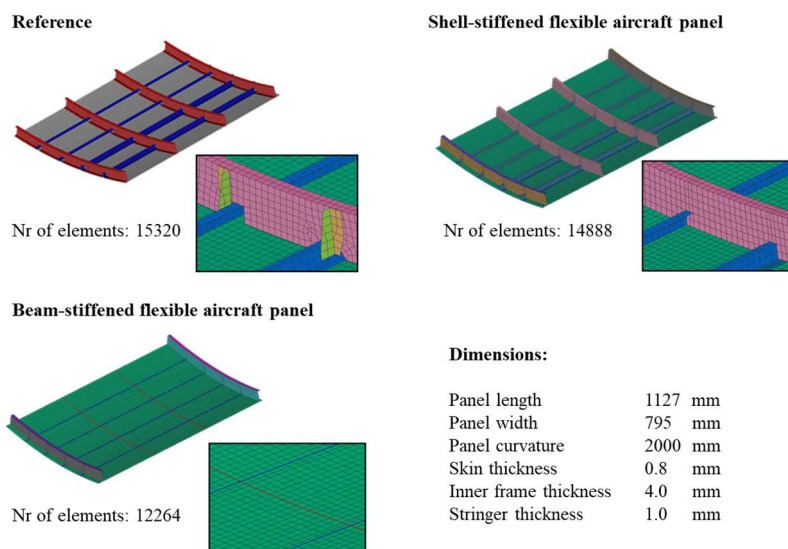


**Figure 1.** Overview of the different models and overall dimensions. The number of elements per model is given.

### 3.3. Mesh size variation

Models with different mesh sizes for the shell-stiffened and the beam-stiffened flexible aircraft panel are studied. Coarser meshes (as for the full aircraft application) are obtained by increasing twice and

four times the mesh size of the reference model. In addition, a finer mesh that has half the reference size is also included. An overview of the mesh sizes and the corresponding number of elements, exemplary for the beam-stiffened panel, is provided in table 3.

**Table 3.** Mesh sizes and number of elements for the beam-stiffened panel.

	Standard	Very coarse mesh	Coarse mesh	Very fine mesh
<b>Mesh size (mm)</b>	10	40	20	5
<b>Nr. of elements</b>	12264	1312	3398	31213

#### 4. Structural model verification

A quasi-static pressure load was considered to assess the influence of the simplifications of the flexible aircraft panel model on the computational results. This analysis was performed with different solvers (implicit and explicit). The load was applied using a pressure versus time tabulated curve. A maximum pressure of 0.1 MPa is reached at 100 ms and kept constant after this time to steady the mechanical response obtained by the explicit solvers. The edges of the panel are fully clamped.

##### 4.1. Reinforcements modelling

The capabilities of the different models were investigated, amongst others, in terms of global panel deformation and local vertical displacement of the nodal position located in the middle of the central bay (node 98534). Two conventional codes used for fast transient dynamic applications (explicit solvers) were used. Reference values are provided by a proprietary FEM implicit solver for quasi-static calculations. Figure 2 shows the contour plot of the global deformation of the shell-stiffened flexible aircraft panel and the vertical displacement time history of node 98534. Symmetric deformation with respect to the X-Z plane is observed as the constant pressure acts on the entirely lateral face of the panel. The outer regions do not deform due to the fact that outer frames are quasi-rigid and are fully clamped. The highest displacement is observed in the central region of the panel, in the position of the node 98534. The maximum vertical displacement over time fits very well for both explicit codes and is in accordance with the reference value.

The results obtained with the beam-stiffened flexible aircraft panel are presented in figure 3. The contour plot of the global deformation is qualitatively similar to the model with the shell reinforcements. The vertical displacement of node 98534 was observed to be higher (8%) for one of the explicit solvers when compared to the shell-stiffened flexible panel. Differences between beam element formulation and integration could contribute to this deviation in the displacement time history and therefore will be further investigated. For the other explicit solver, a very good agreement between both discretization types was addressed. Similar findings are observed for the central nodes of the front (node 51679) and the aft (node 145389) panel bay. In general, the response of the flexible panel with beam reinforcements shows important similarities when comparing with the model with shell reinforcements under the same loading condition.

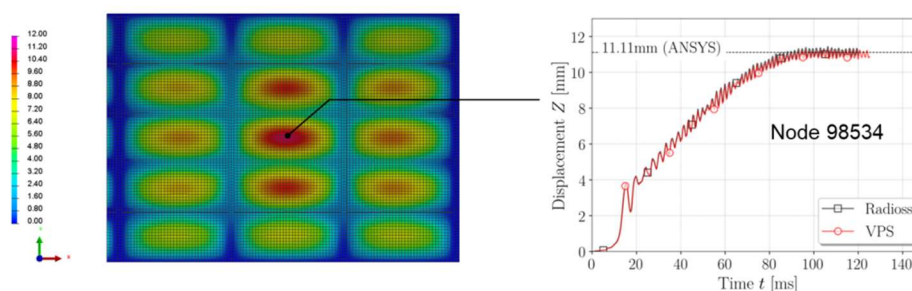


**Figure 2.** Shell-stiffened flexible panel. Left: global deformation in mm at 100 ms. Right: displacement in vertical direction of the central node.



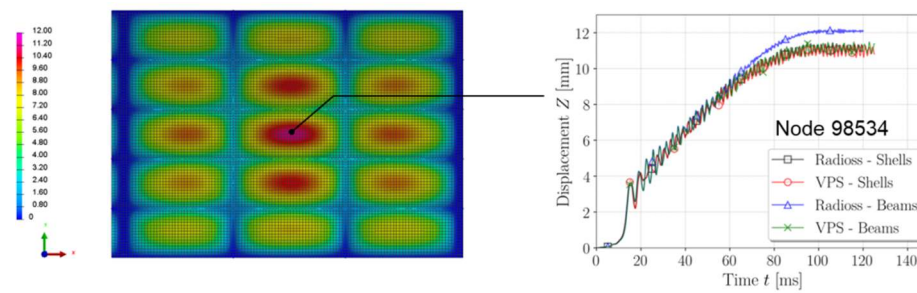


**Figure 3.** Beam-stiffened flexible panel. Left: global deformation in mm at 100 ms. Right: displacement in vertical direction of the central node.

#### 4.2. Mesh size variation

Computations with the different mesh sizes presented in table 3 were undertaken with the explicit solver VPS for both the shell-stiffened and the beam-stiffened flexible panel model. Figure 4 shows the contour plot of the global deformation obtained for the very coarse mesh models and the vertical displacement time history of the central node of the panels. Similar responses were observed compared to the models with the standard mesh size. The time history of the displacement in z-direction predicts good agreement with previous findings. Only the shell-stiffened flexible panel with a very fine mesh size exhibits slightly higher displacements. To conclude, the capability of beam models (instead of shell elements) to model aircraft panel reinforcements was demonstrated with this quasi-static loading condition.

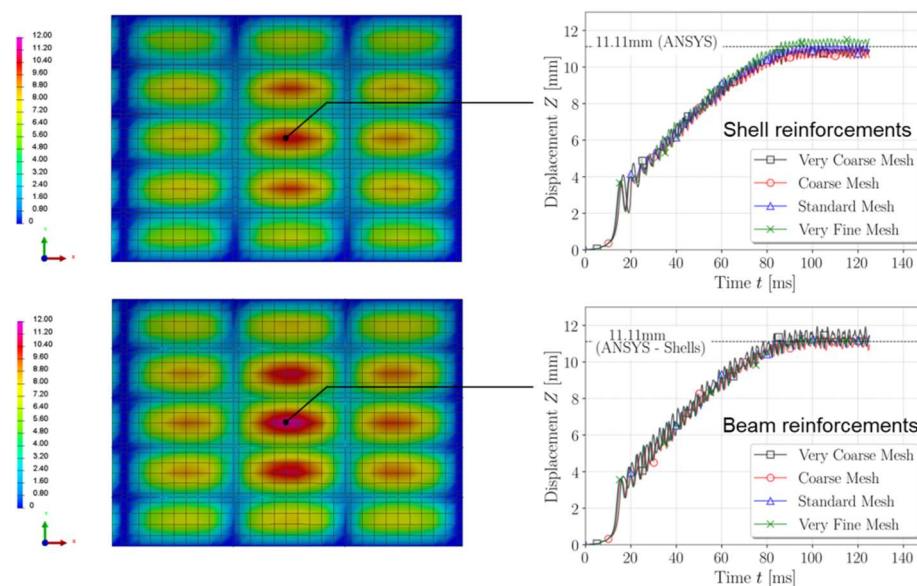


**Figure 4.** Global deformation in mm at 100 ms and displacement in vertical direction of the central node for all mesh sizes. Top: shell-stiffened flexible panel. Bottom: beam-stiffened flexible panel. The position of the central node differs slightly due to the mesh size variation.

### 5. Application in a guided ditching simulation

The flexible aircraft panel was used for guided ditching simulations. The panel impacts the fluid with a sink rate of  $1.5 \text{ ms}^{-1}$ , a forward velocity of  $40 \text{ ms}^{-1}$ , and a pitch angle of  $6^\circ$ . The length, width and height of the water basin are 5 m, 1 m and 0.2 m, respectively. In total, the simulation time of the guided ditching is 85 ms, which covers the impact and the initial landing phases of the ditching. Computational results obtained with the coupled SPH-FE and the ALE-CEL approaches are compared for simulations with the shell-stiffened flexible panel model. In addition, guided ditching simulations with the beam-stiffened flexible panel model are considered and complemented with simulations using different mesh sizes and corresponding particle densities.

### 5.1. Application with different computational methods

In figure 5 global results of the guided ditching simulation with the shell-stiffened flexible panel are portrayed. The images on the left side show the contour plots of the fluid pressure at 25 ms, when the central bay of the panel enters in contact with the fluid surface. The top picture, related to the simulation with the ALE-CEL formulation, shows lower fluid pressure levels compared to the simulation using the coupled SPH-FE approach, presented in the bottom. Consequently, global deformation is higher in the case of the SPH-FE computation. Figure 5 also compares the equivalent stress field observed on the structure at 60 ms (all bays of the panel are in contact with the fluid) with the ALE-CEL and the SPH-FE approaches (center and right side, respectively). Local stresses are slightly higher in the case of the SPH-FE computation.

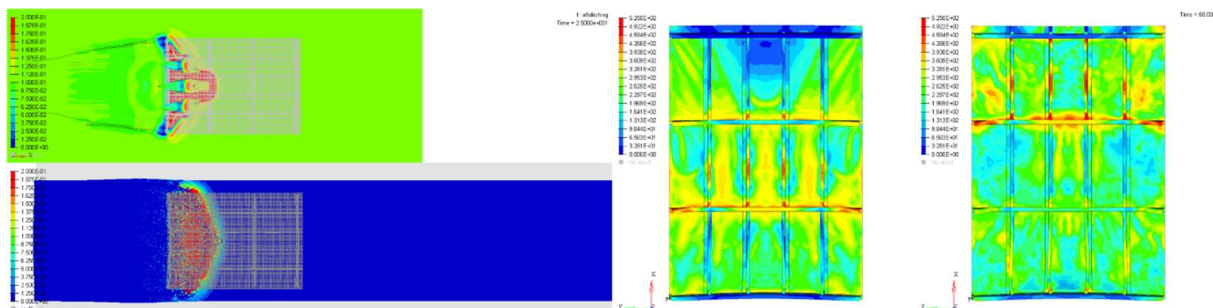


**Figure 5.** Guided ditching simulation of the shell-stiffened panel. Contour plot of the fluid pressure in MPa (Top: ALE-CEL. Bottom: SPH-FE). Contour plot of the structural stresses in MPa (Center: ALE-CEL. Right: SPH-FE).

To investigate the local responses of the flexible panel, shell elements were selected in frame-stringer and skin-stringer intersections located in the panel bay which experiences the initial interaction with the fluid. Figure 6 shows the position of these elements and the maximum von Mises stress time histories obtained with the ALE-CEL and the SPH-FE approaches. In general, higher stress levels were observed for the simulation based on the coupled SPH-FE approach. For elements in the frame-stringer intersection maximum stress is reached in the period between 15 and 30 ms, thus experiencing the highest amount of plastic deformation. The capacity of the stringer to withstand the hydrodynamic loading is reduced (collapse of the reinforcements), which is assumed to explain the overall higher deformation in the central and the front panel bay, compared to simulations using the ALE-CEL formulation.

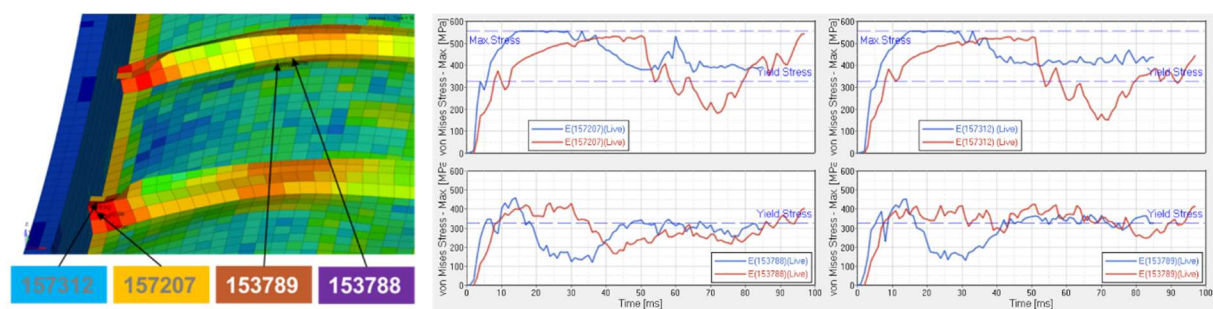


**Figure 6.** Location and the maximum von Mises stress time history in MPa for selected elements in the rear bay of the shell-stiffened flexible panel. Blue curves: SPH-FE. Red curves: ALE-CEL.

Figure 7 compares the time history of the vertical force obtained with the SPH-FE and the ALE-CEL computations. The responses denote noticeable differences. However, the maximal force level obtained with both computational approaches was similar.

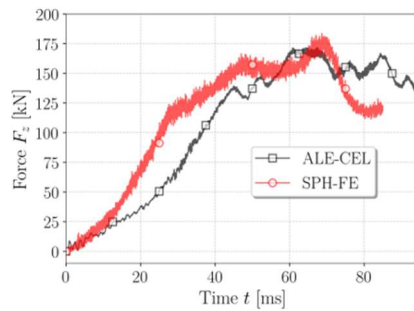


**Figure 7.** Vertical force time history of the shell-stiffened flexible aircraft panel with the coupled SPH-FE and the ALE-CEL methods.

### 5.2. Modelling transfer

FE models developed with simple beam finite elements for the skin reinforcements are used to simulate the guided ditching of the flexible panel with the SPH-FE approach. Figure 8 shows the contour plot of the SPH particle pressure for the shell-stiffened and the beam-stiffened flexible panel (left), and the contour plot of the equivalent stress field on the shell-stiffened and the beam-stiffened flexible panels (center and right side, respectively). In general, the results are qualitatively similar and both the fluid domain and the structure exhibit a comparable behavior at this instant (50 ms).

The interaction between fluid domain and the flexible panel was analyzed in terms of contact force in vertical direction. Figure 9 shows the time history of the total vertical forces for the shell-stiffened and beam-stiffened models and the reference model (left). A very good agreement between models can be observed, considering all simplifications conducted in the model of the structure. Further, divergences between the beam-stiffened and the shell-stiffened flexible panel are very limited.

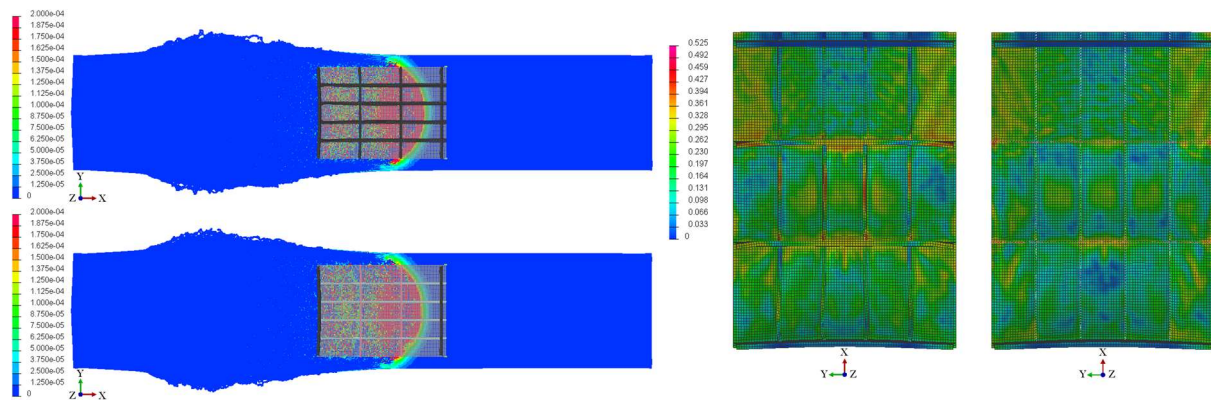


**Figure 8.** Comparison of the guided ditching simulation at 50 ms with different panel models. Contour plot of the fluid pressure in GPa (Top: Shell-stiffened flexible panel. Bottom: Beam-stiffened flexible panel). Contour plot of the structural stresses (shell elements) in GPa (Center: Shell-stiffened flexible panel. Right: Beam-stiffened flexible panel).



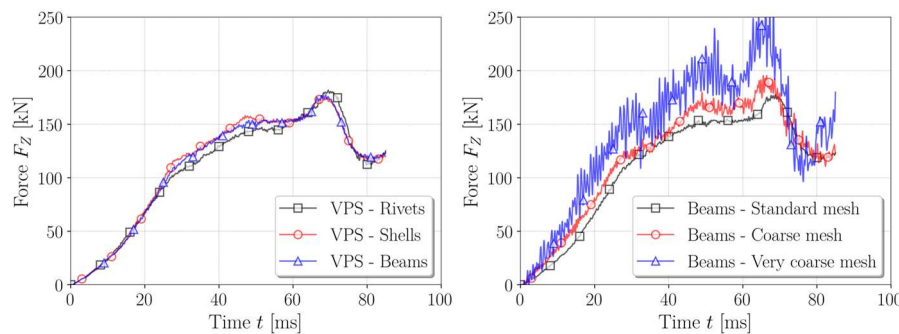


**Figure 9.** Vertical force time history. Left: reference, shell-stiffened and beam stiffened flexible panel. Right: beam-stiffened flexible panel with different mesh sizes.

Figure 9 also shows the time history of the contact force in vertical direction for the beam-stiffened flexible aircraft panel with different mesh sizes (right). In general, the results are comparable, specially between the models with the standard and the coarse mesh size. The contact force curve shows a similar tendency for all the cases. The computational elapsed time was reduced by factor 15 in the case of the panel with the coarse mesh size compared to the standard model. Thus, coarser meshes could be implemented for the flexible panel in guided ditching simulations, reducing the complexity of the model and showing a significant saving of computational effort in terms of time.

Results show the feasibility and capability of the beam element reinforcements modelling technique in ditching applications.

## 6. Conclusions

The possibility to represent typical aircraft structures like stringers and frames by using simple beam representations in reinforced aircraft fuselage panels for guided ditching applications to reduce model complexity and computational effort was assessed in this work. Further developments with reduced model complexity as well as with different mesh sizes were investigated with a constant quasi-static pressure loading condition, resulting in a general good agreement between models and codes. Subsequently, the models were used for guided ditching simulations. The investigation included the coupled SPH-FE and the ALE-CEL formulations and comparisons between different models, showing the feasibility to use beam elements for structural reinforcements in flexible aircraft panels with different mesh sizes in ditching simulations.

## References

- [1] EASA 2014 Certification specifications and acceptable means of compliance for large aeroplanes CS-25/Amdt 15 *EASA Tech. Rep.*
- [2] Siemann M 2016 Numerical and experimental investigation of the structural behavior during aircraft emergency landing on water *DLR F. B.*
- [3] Siemann M, Kohlgrüber D and Voggenreiter H 2017 Numerical simulation of flexible aircraft structures under ditching loads *CEAS A. J.* 8 pp 505–21
- [4] Langrand B, Siemann M, Kohlgrüber D and Leon Muñoz C 2019 Full aircraft ditching simulation by advanced fluid structure interaction computational methods: a comparative analysis *ASIDIC (Madrid)*
- [5] Leon Muñoz C, Kohlgrüber D and Petsch M 2019 Aircraft Ditching Simulations within a Multi-disciplinary Aircraft Design Process Chain *ESI-Forum (Berlin)*
- [6] Gingold R A and Monaghan J J 1977 Smoothed particle hydrodynamics - Theory and application to non-spherical stars *Mon Not Roy Astron Soc* 181 pp 375–89
- [7] Siemann M and Langrand B 2017 Coupled fluid-structure computational methods for aircraft ditching simulations: comparison of ALE-FE and SPH-FE approaches *Computers & Structures* 188 pp 95–108
- [8] Donea J, Huerta A, Ponthot J P and Rodríguez-Ferran A 2004 Arbitrary lagrangian-eulerian methods *Encyclopedia of Computational Mechanics* (New Jersey: John Wiley & Sons)